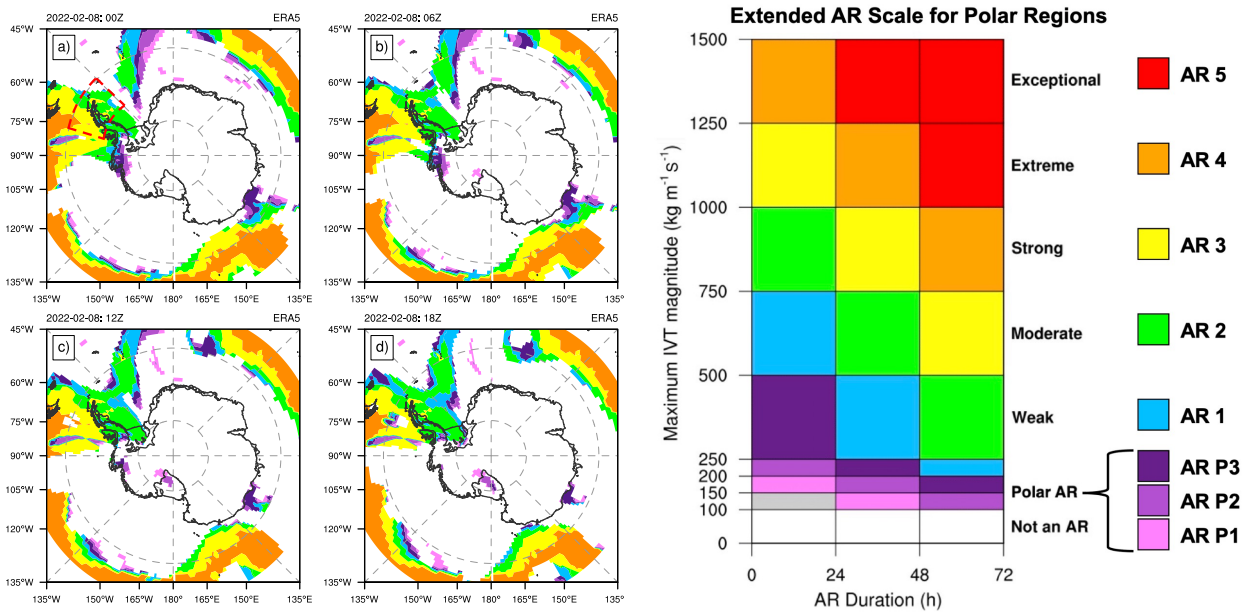

Fig. S1. Gridded Enhanced AR Scale developed based on the duration of AR and the maximum integrated water vapor transport in the duration at each grid point. (a-d) gridded Enhanced AR Scale for an AR3 event over the AP in February 2022[1]. The red dashed box in a) highlights the area used for the averaged gridded Enhanced AR scale calculation. This gridded dataset is calculated based on ERA5 reanalysis dataset.

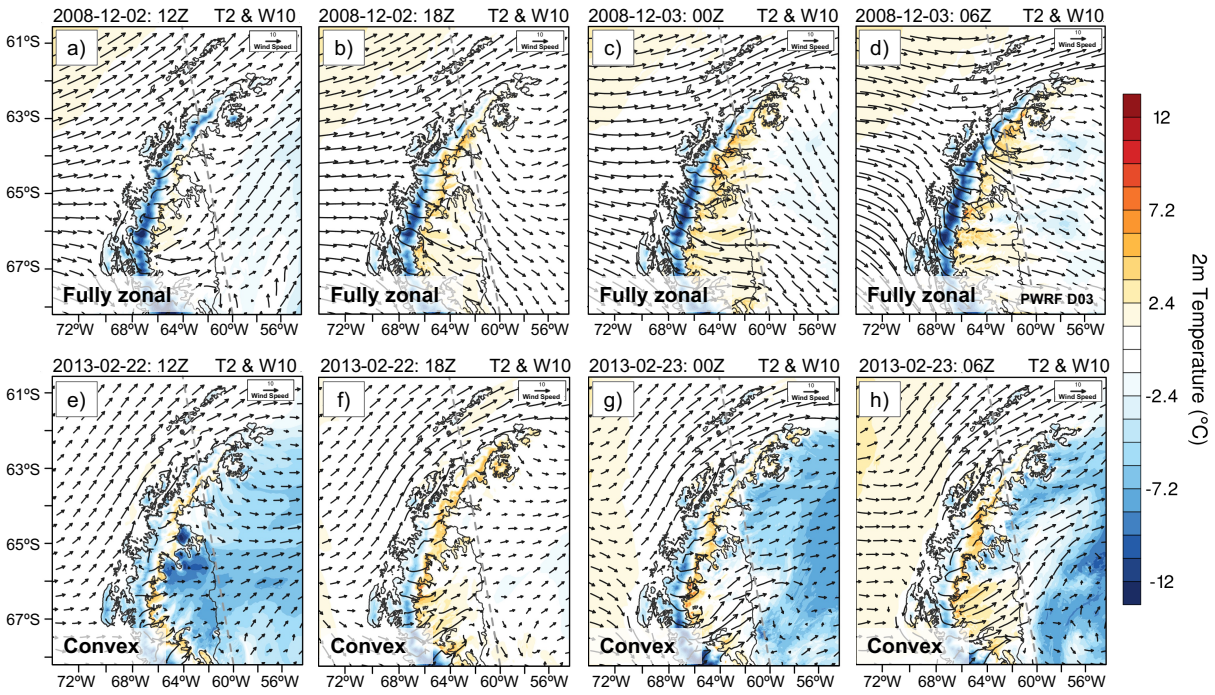

Fig. S2. Evolution of 2 m temperature (T2; shading; °C) and 10 m wind (W10; vectors; m s^{-1}) of (a-d) fully zonal and (e-h) convex AR events, occurring in December 2008 and February 2013 respectively, and based on PWRF simulations. (a-d) shows results at 12Z 2 Dec, 18Z 2 Dec, 00Z 3 Dec, and 06Z 3 Dec, respectively. (e-h) shows results for 12Z 22 Feb, 18Z 22 Feb, 00Z 23 Feb, and 06Z 23 Feb, respectively. The length of the reference arrow at the lower right corner of each panel represents a wind speed of 10 m s^{-1}.

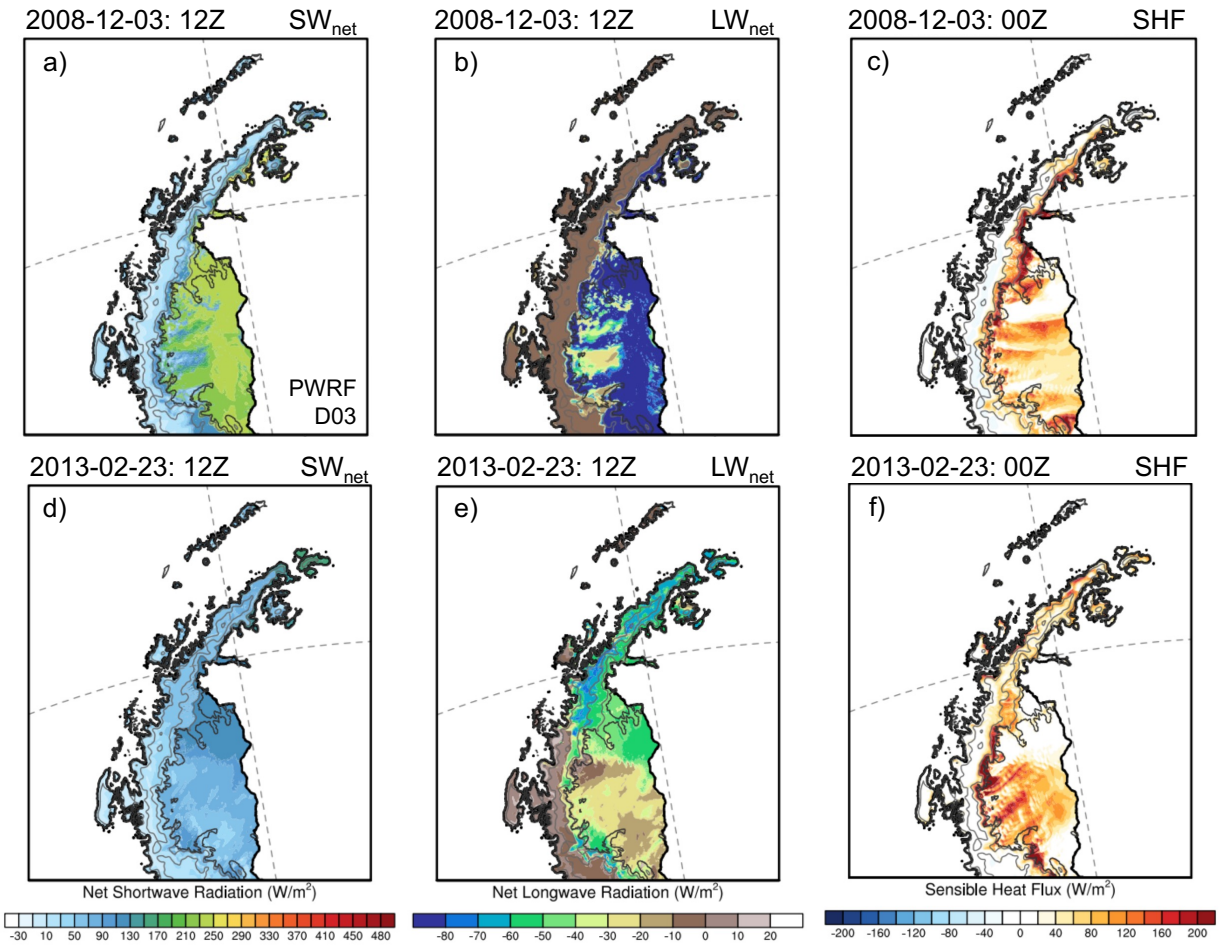

Fig. S3. Surface energy balance components (W m^{-2}) of (a-c) fully zonal and (d-f) convex events, occurring in December 2008 and February 2013 respectively, and based on PWRF simulations. (a,d) net shortwave radiation (SW$_{net}$; W m^{-2}), (b,e) net longwave radiation (LW$_{net}$; W m^{-2}) at 12Z 03 Dec and 12Z 23 Feb, and (c,f) sensible heat flux (SHF; W m^{-2}) at 00Z 03 Dec and 00Z 23 Feb.

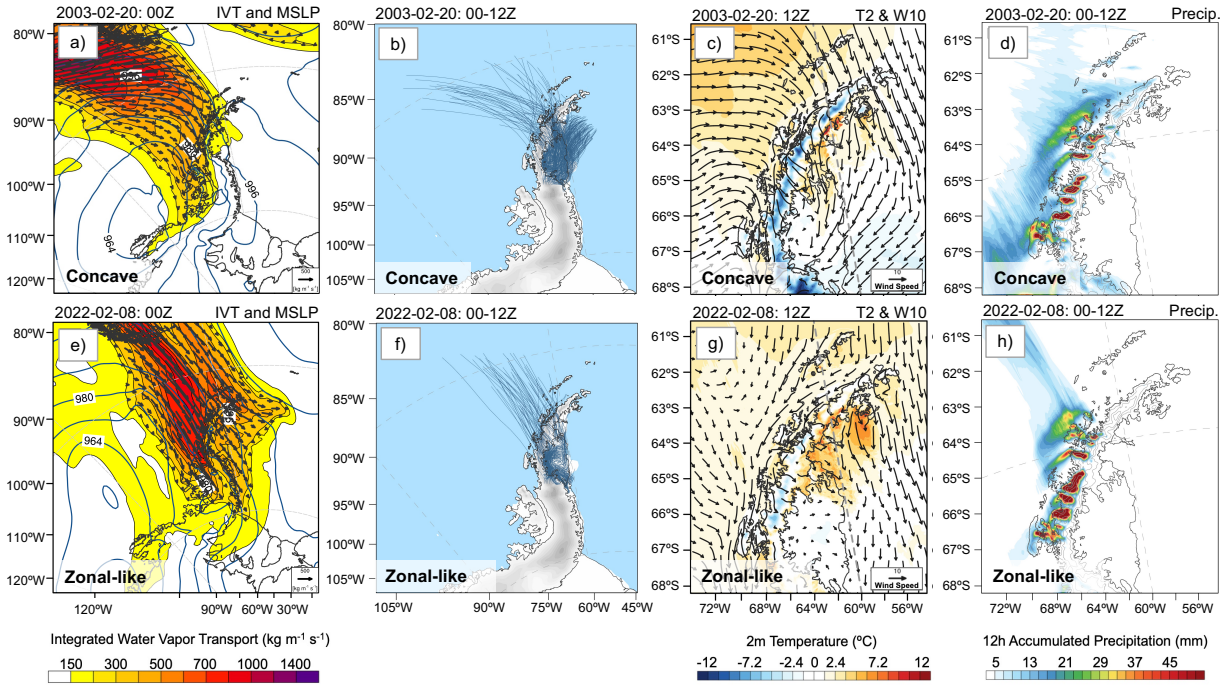

Fig. S4. As Fig. 5 but showing (a-d) concave and (e-h) zonal-like AR events, occurring in February 2003 and February 2022, respectively, and based on PWRF simulations. (a,e) Integrated Vapor Transport (IVT; shading; kg m^{-1} s^{-1}) and Mean Sea Level Pressure (MSLP; contours; hPa) at 00Z on 20 Feb and 8 Feb, respectively. (b,f) 12-hour back trajectories ending over the LCIS from 00 to 12Z on 20 Feb and 8 Feb, respectively. (c,g) 2 m temperature (T2; °C) and 10 m wind fields (W10; m s^{-1}) at 12Z on 20 Feb and 8 Feb, respectively. (d,h) 12h accumulated precipitation (Precip; mm) from 00 to 12Z on 20 Feb and 8 Feb, respectively. The length of the reference arrow in (c,g) represents a wind speed of 10 m s^{-1}.

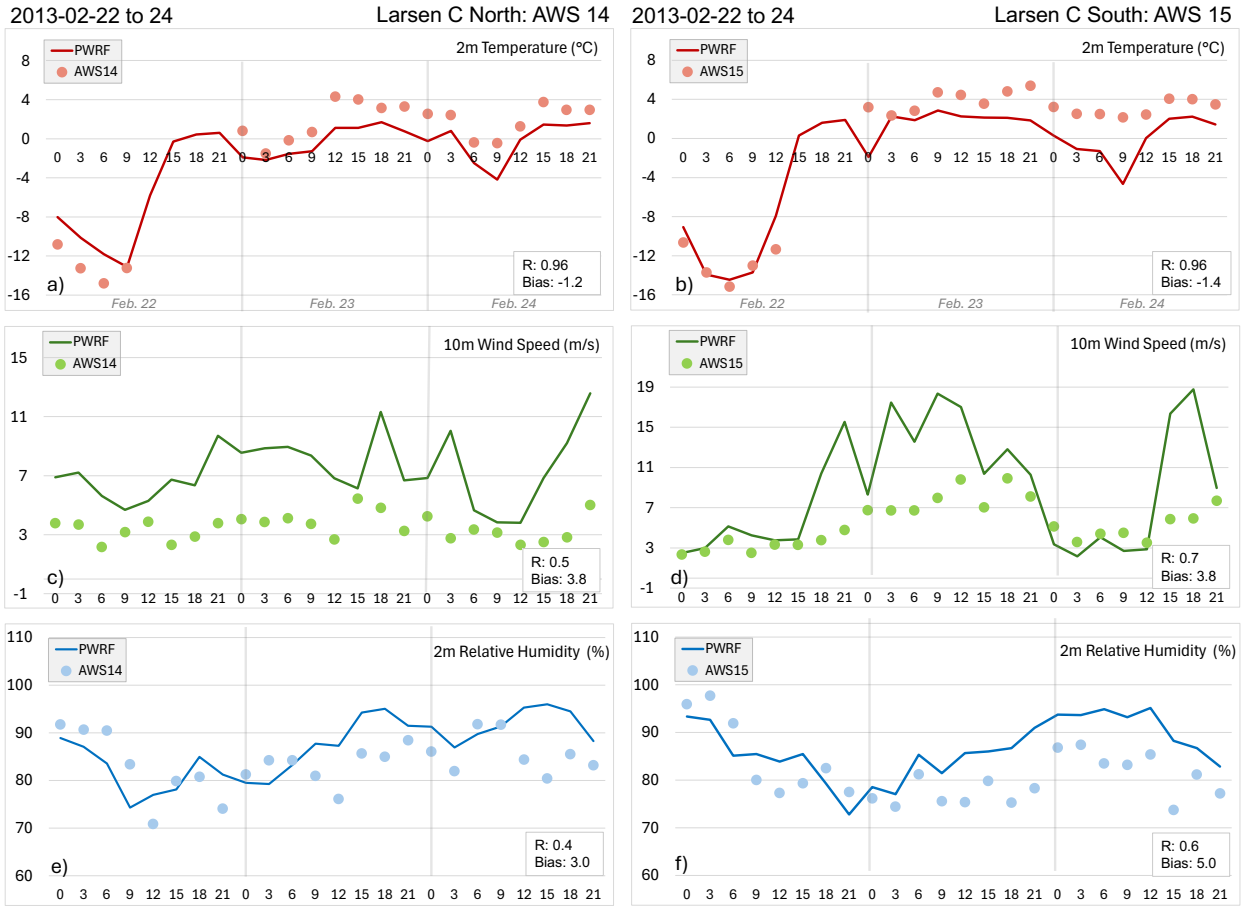

Fig. S5. Comparison of PWRF simulations and Automatic Weather Stations (AWS) observations for a convex AR event occurring in February 2013. (a-b) 2 m temperature (T2; °C), (c-d) 10 m wind speed (W10; m s^{-1}), and (e-f) 2 m relative humidity (RH2; %) comparison at AWS15 and AWS14 over the LCIS from 00Z 22 to 24 Feb 2013. Locations of AWS14 and AWS15 are marked with red crosses in Fig. 1.

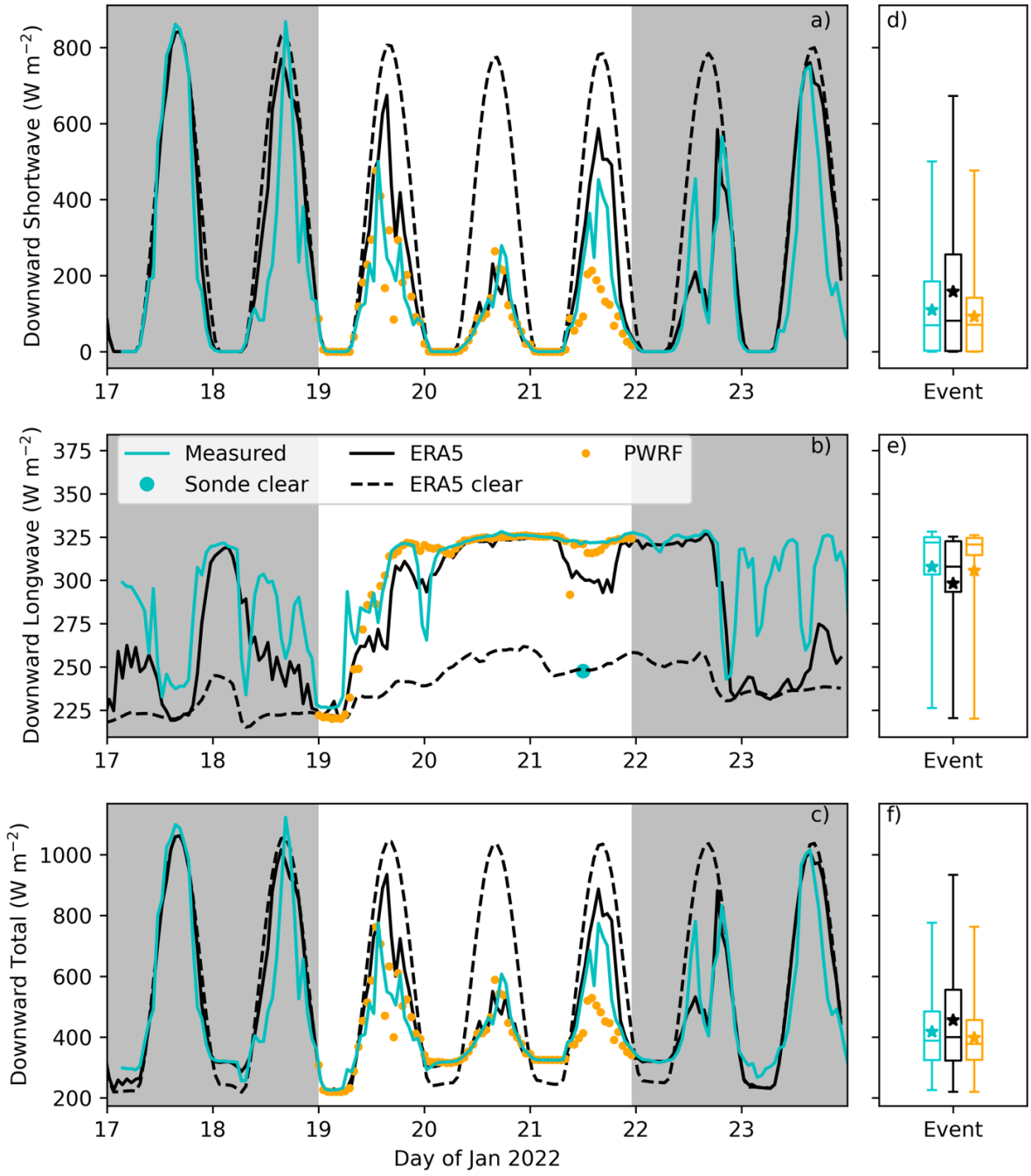

Fig. S6. Time series of downward longwave and shortwave fluxes at the surface at Escudero Station on King George Island during a combined AR-föhn event from 19 to 21 January 2022. (a-c) observations (measured; averaged hourly), clear-sky simulations based on radio sounding measurements (Sonde clear), sky-view and clear-sky results from ERA5 (ERA5 and ERA5 clear) and sky-view results from PWRF simulations. The AR duration is shown as the white span. (d-f) statistics for the duration of the AR event (white span in panels a-c), where the asterisk indicates the mean, the horizontal bar the median, the boxes the interquartile range, and the whiskers the full range. The legend in panel b corresponds to all panels.

Table S1. List of AR events impacting the AP during austral summers since December 2001[2].

Case	Start Date	End Date	Duration (days)	AR Scale (ERA5)
1	2001-12-12	2001-12-15	4	AR2
2	2002-01-01	2002-01-02	2	AR1
3	2002-02-07	2002-02-08	2	AR1
4	2002-02-24	2002-02-26	3	AR2
5	2002-12-11	2002-12-16	6	AR2
6	2003-02-19	2003-02-21	3	AR1
7	2004-02-08	2004-02-10	3	AR1
8	2005-01-03	2005-01-05	3	AR2
9*	2005-02-08	2005-02-16	9	AR3
10	2006-01-21	2006-01-24	4	AR2
11*	2006-02-06	2006-02-12	7	AR1
12	2008-01-24	2008-01-27	4	AR2
13	2008-02-23	2008-02-24	2	AR1
14	2008-12-01	2008-12-03	3	AR2
15	2011-02-23	2011-02-24	2	AR2
16	2011-02-26	2011-02-28	3	AR2
17	2011-12-04	2011-12-06	3	AR2
18	2011-12-15	2011-12-17	3	AR3
19	2013-02-22	2013-02-24	3	AR2
20	2014-02-15	2014-02-17	3	AR1
21	2014-02-24	2014-02-26	3	AR2
22	2015-01-28	2015-01-29	2	AR1
23	2015-02-05	2015-02-06	2	AR1
24	2016-01-01	2016-01-04	4	AR2
25	2016-01-29	2016-01-30	2	AR2
26	2016-02-06	2016-02-08	3	AR2
27	2016-02-20	2016-02-22	3	AR2
28	2018-02-21	2018-02-23	3	AR1
29	2019-02-04	2019-02-05	2	AR2
30	2020-02-04	2020-02-10	7	AR3
31*	2021-02-08	2021-02-14	7	AR3
32	2021-02-27	2021-03-01	3	AR2
33	2021-12-08	2021-12-10	3	AR2
34	2021-12-17	2021-12-19	3	AR3
35	2022-01-19	2022-01-21	3	AR2
36	2022-02-01	2022-02-03	3	AR2
37	2022-02-07	2022-02-09	3	AR3
38	2022-02-20	2022-02-24	5	AR2

*indicate AR-family events, and the AR Scale represents the maximum scale detected on the upwind side of the LCIS.

Table S2. Summary of all AR-föhn patterns affecting the LCIS.

AR-föhn Patterns	Circulation	Impact Area	Representative Case
Zonal-like	High-low coupled system	Northern Larsen C	2022-02-06 to 09
Fully zonal	High-low coupled system	North Larsen C, and mountain foothills	2008-12-01 to 03
Concave	Low pressure system	Northern Larsen C	2003-02-19 to 21
Convex	High pressure system	Entire Larsen C	2013-02-22 to 24

Table S3. PWRF model settings.

	PWRF V4.3.3
Input Data	ECMWF Reanalysis Data (ERA5)
Horizontal Resolution	30 km / 6 km / 1.2km
Vertical levels	71 levels (lowest level 4m above the surface)
Temporal Resolution	hourly
Spin-up	24 h
Microphysics	P3
PBL Scheme	MYNN
Shortwave and Longwave	Both RRTMG
Land Surface Options	Noah MP
Surface Layer Options	MYNN
Surface Albedo	MODIS observed surface albedo (MCD43C3)
High-Res Topo	Reference Elevation Model of Antarctica (REMA)1km topo
Nudging	Every 6 hours; nudging to u, v wind, temperature and water vapor from ERA5 for model level 40 (~400 hPa) and above.

References:

1. Zou, X. *et al.* Strong Warming over the Antarctic Peninsula during Combined Atmospheric River and Foehn Events: Contribution of Shortwave Radiation and Turbulence. *J. Geophys. Res. Atmos.* **128**, e2022JD038138 (2023).
2. Zou, X. *et al.* Selected austral summer Atmospheric River cases over the Antarctic Peninsula, 2001 - 2022. Antarctic Meteorological Research and Data Center https://doi.org/10.48567/exak-2810 (2025).